Beamforming in the Body: Energy-efficient and Collision-free Communication for Implants

[1]Meenupriya Swaminathan, [2]Anna Vizziello, [3]Davy Duong, [4]Pietro Savazzi and [5]Kaushik R. Chowdhury,
[1,5]Electrical and Computer Engineering Department, Northeastern University, Boston, MA, USA.
[2,4]Department of Electrical, Computer and Biomedical Engineering, University of Pavia, Pavia, Italy
[3]Electrical and Computer Engineering department, Temple University, Philadelphia, PA, USA
E-mail:{[1]meenu, [5]krc}@ece.neu.edu, {[2]anna.vizziello, [4]pietro.savazzi}@unipv.it, [3]davyduong@temple.edu

Abstract—**Implants are poised to revolutionize personalized healthcare by monitoring and actuating physiological functions. Such implants operate under challenging constraints of limited battery energy, heterogeneous tissue-dependent channel conditions and human-safety regulations. To address these issues, we propose a new cross-layer protocol for galvanic coupled implants wherein weak electrical currents are used in place of classical radio frequency (RF) links. As the first step, we devise a method that allows multiple implants to communicate individual sensed data to each other through CDMA code assignments, but delegates the computational burden of decoding only to the on-body surface relays. Then, we devise a distributed beamforming approach that allows coordinated transmissions from the implants to the relays by considering the specific tissue path chosen and tissue heating-related safety constraints. Our contributions are two fold: First, we devise a collision-free protocol that prevents undue interference at neighboring implants, especially for multiple deployments. Second, this is the first application of near-field distributed beamforming in human tissue. Results reveal significant improvement in the network lifetime for implants of up to 79% compared to the galvanic coupled links without beamforming.**

I. INTRODUCTION

Assistive technologies allow humans to augment their natural abilities and restore physiological functions lost due to illness or injury. An example of today's closed loop communication with man-machines interfaces involves controller-driven artificial limb stimulation based on muscle exertion levels. Embedded sensors in the tissue detect the muscle stress and communicate their readings back to the controller for precisely computing the needed stimuli for limb movement [1]. This paradigm of interconnected implants results in an Intra-Body Network (IBN) that allows internal physiological data to be gathered in real time and analyzed off site, thereby transforming personalized medicine. However, the state of the art for intra-body communication relies on high frequency radio (RF) signals. RF incurs significant energy costs owing to high absorption within the human tissues that are composed of 40-65% water. Additionally, emitted RF signals may extend to several feet around the body, creating privacy risks. We use an alternative wireless architecture for IBNs using galvanic coupling (GC), in which low or medium frequency ($100\,\mathrm{kHz}$-$1\,\mathrm{MHz}$) and weak ($\leq 1\,\mathrm{mW}$) electrical currents are modulated with data and directly coupled to the tissue. We

call this paradigm as GC-IBN, and it consumes two orders of magnitude less energy than RF signals [2].

● **Problem:** The GC-IBN architecture is composed of multiple embedded implants that transmit their sensed data to an on-skin node, called as a *relay*. The muscle to muscle (M-M) path offers lowest pathloss (≈ 19 dB) and hence, is ideally suited for communication across different implants in the same muscle layer [2]. However, implant to the surface relay communication needs to traverse several different tissue boundaries that have higher path loss, for e.g, the muscle to skin (M-S) path has ≈ 38 dB of loss. How to send these signals to the relay with the least overhead (even if the baseline GC performance is much more energy efficient than RF) with high SNR remains an open challenge [3], [4]. Further, existing standards like IEEE 802.15.6 designed for implant communication use contention-based medium access with the possibilities of collisions, backoff and packet loss. Such events incur energy costs of re-transmissions and idle-listening, which we wish to avoid in IBNs.

● **Proposed Approach:** We propose a light-weight cross-layer framework that combines code division multiple access (CDMA) with distributed beamforming in narrow band channels, while ensuring that computational costs are delegated to the relay. The implants themselves simply record and forward data, with the relay being responsible for both the CDMA decoding (to extract the actual sensed value) and tuning of the beam-steering matrix (for directional communication with high SNR). Existing far-field beamforming techniques cannot be applied for GC-IBN, as the receiver is placed in the near-field of the low frequency transmitter, separated only by a few tens of centimeters. The complete procedure is described as follows: The relay assigns unique CDMA codes to the implants. The latter store the sensed values and create modulated codewords using these assigned orthogonal codes. Using the high-gain M-M channel, the implants inform a designated aggregator, placed in the same muscle tissue, of their individual codewords. Such aggregator records the received CDMA-coded data structure created by the simultaneous transmissions of multiple sensors on the same channel. Note that there is no decoding step at this point to save energy, and the aggregator simply broadcasts back this cumulatively received codeword to the implants. By using distributed beam-

forming, each implant then transmits this codeword to the relay. Through this process, the energy consumed per implant is reduced, greater directional transmission is obtained and the relay receives much higher SNR than what would have been possible via a single sensor transmission. The final CDMA decoding is then performed at the relay, and the individual sensor data is then extracted. The entire 2-step process of (i) exchanging individual codewords among peer implants, and (ii) beamforming to the relay, is collision-free.

• **Contributions:** The main contributions of this work are:

1. We propose a CDMA-based cross-layer approach that allows implants in the muscle to communicate with surface relays using galvanic coupling, which is collision-free and has reduced complexity of decoding.

2. We present the first formulation of near-field distributed beamforming in the body that accounts for specific tissue paths, constraints of tissue safety ($\leq 25\,mA/m^2$) [4] and increases SNR at the surface relays. We present tissue-phantom and Arduino-based proof-of-concept experimental study of how constructive phase addition is possible within the body.

3. We use empirically obtain data sets to model the body channel and evaluate the effectiveness of our approach using an extensive finite element based simulation using MATLAB-generated mathematical models.

The rest of the paper is organized as follows: Sec.II describes the related contributions, and the initial motivation using experiments is presented in Sec.III. The beamforming technique is explained in Sec.IV. Sec.V describes the modified CDMA scheme. We provide rigorous performance evaluation studies in Sec.VI. Finally, Sec.VII concludes the paper.

II. BACKGROUND AND RELATED WORK

Existing standards for Wireless Body Area Communication (WBAN), including IEEE 802.15.4 based LR-WPAN (Zigbee), IEEE 802.15.6 Human Body Communication (HBC) standard and Bluetooth low energy (BLE), assume that implants are similar to classical over-the-air wireless sensors. This is because in both cases, the nodes are battery powered, have small form factors, with low on-board resources. Classical CSMA/CA [5], [6] and channel hopping used in these standards impacts definite time of delivery, energy efficiency, and is unable to handle sudden spikes in traffic. The frame-length and inter-frame spacing are designed for high frequency signal propagation in the air medium over long distances ($>>2\,m$), rather than the low frequency short range communication ($< 50\,cm$) inside the body. Other overheads such as handshakes, channel sensing, scheduling, transitions from frequent sleep and wake-up states, among others, increase the processing complexity. An alternative form of intra-body links established using ultrasonic signals suffer from high multi-path delay and complex circuitry.

We note that the low rate and sparse traffic generated by implants under normal physiological conditions may become bursty when an abnormal event is observed, limiting utility of both contention-based and reservation-based access techniques. Hence, for contention and reservation-free access, we advocate the use of [7] that enables concurrent transmissions. However, CDMA multiplies the energy costs by using a high rate code, which in turn contributes to the net energy consumed per unit of useful data. Hence, in this paper we design smart energy-focusing strategies. Seminal contributions for conventional beamforming in far-field, high frequency signals exist [8]. However, the problem of beamforming for near-field and narrow band signals in a heterogeneous tissue-like medium has not been demonstrated so far, particularly for the low frequency signals (<1 MHz) used in GC-IBN. Coordinated beamforming using multiple separate antenna elements may be possible in many applications where implants are placed in close proximity of each other, such as for neuro-muscular stimulation or orthopedic sensors that merits further investigation on this topic [1], [9].

III. TISSUE PHANTOM EXPERIMENTS

As a motivation for choosing beamforming, we use a tissue phantom-based testbed (see Fig. 1(a) for the block diagram describing the setup and Fig. 1(c) for a snapshot) to analyze the constructive and destructive combination of concurrently propagating signals through tissue. We use pulse width modulated (PWM) signals at $100\,kHz$ and $0.5\,V$ generated by a pair of Arduino Uno boards, whose phase is controlled by a common synchronization pulse generated by MATLAB. The PWM signals are passed through a safety circuit (Fig. 1(b)) in order to limit the signal within the safe bound (=1 mA) we set based on the suggestion by ICNIRP [4] and then coupled to the muscle phantom (mimicking implants) by two pairs of electrodes. The transmitters are separated by $16\,cm$ and the electrode pair in each transmitter is separated by $4\,cm$. A pair of receiving electrodes is positioned on the surface skin of the phantom at $15\,cm$ from each transmitter, and connected to an oscilloscope to observe the output voltage. For each signal, the corresponding Thevenin-equivalent circuit is built to measure the output power level.

When only one Arduino is transmitting a power of $0.25\,mW$, the maximum average output power (Pr_{max}) we observed is $3\,\mu W$. When two transmitters are transmitting concurrently, and in perfect phase alignment (Fig 1(d)), Pr_{max} is $6\,\mu W$, which is double than the case of a single transmitter. This shows that the constructive signal addition is beneficial. However, when the input signals are out of phase (Fig 1(e)), $Pr_{max} \approx 2.6\,\mu W$, which is lower than the case of a single active transmitter, showing the impact of destructive signal combination. When the signals are partially out of phase (Fig. 1(f)), Pr_{max} becomes $\approx 4.3\,\mu W$. The set-up includes the mutual coupling effect from multiple transmitters and thus mimics the real scenario. Our experiments motivate the potential benefits of phase-alignment based beamforming within heterogeneous tissues using GC-coupled links.

IV. BEAMFORMING FOR IMPLANT COMMUNICATION

In this section, we first develop the formulations for near-field beamforming that will be used within the tissues. We start the discussion assuming each implant has a common CDMA
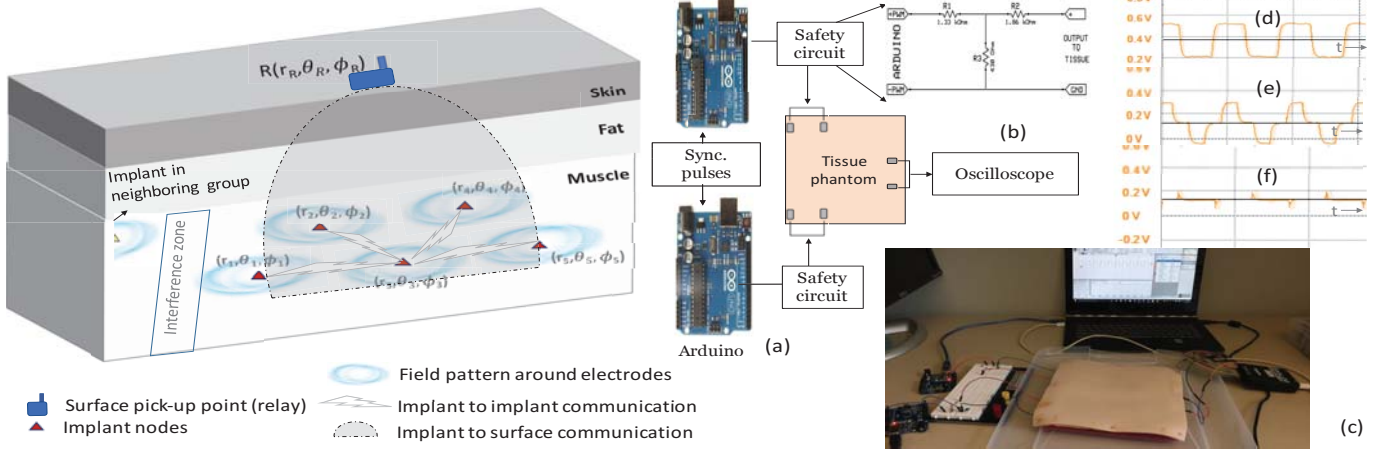
Fig. 1. (left) Human fore-arm GC-IBN with muscle implants and surface relay; (right) Phantom-based testbed using Arduino

modulated codeword $\mathbf{D}'$, created and disseminated by the aggregator back to the implants. The steps through which this vector $\mathbf{D}'$ is constructed from the individual sensed values is explained in Sec. V. The idea here is to let the set of implants collectively act as a distributed antenna array and improve the directional emission of the near-field transmission towards the relay, while minimizing its propagation in other undesired directions. Our method requires manipulating the signal transmitted from each implant in amplitude and phase using complex weights. Hence, we first explain the requirement for near-field analysis in Sec.IV-B and derive the electromagnetic field pattern of each implant in Sec.IV-C. We extend the near-field analysis to the array-structure resulting from multiple nearby implants, and then calculate the cumulative received power at the surface relay in Sec.IV-D. Then, we derive the complex weights to limit the beamformed signal within the safe power limit, focus the signal strength at the receiver and devise a method to steer the input signals from each node in the desired direction in Sec.IV-E.

A. Network architecture and 3-D tissue channels

We assume a set of M uniformly distributed co-planar implants $\{m_1,..,m_M\}$ arranged in muscle tissue linearly, at

TABLE I
VARIABLE DEFINITIONS AND RANGES

Variables	Definitions
M, R & m_i	Total number of nodes, Relay & Implant i
M-M, M-S, S-M	Paths: Muscle-muscle, muscle-skin, Skin-muscle
$\overrightarrow{H}, \overrightarrow{E}$	Instantaneous magnetic and electric fields
θ_i, ϕ_i	Azimuth and elevation angles
r_i	Distance between 2 points in spherical coordinates
AF	Array factor
g^p	Gain in path p; ge - $\overrightarrow{E}$ gain; gh - $\overrightarrow{H}$ gain
ψ, γ	Phase shift and Frequency offset
$f, w, \triangle f$	Frequency, angular frequency and bandwidth
$c \& c'$	Speed of EM signals in vacuum and tissue
w^s, w^p, w^t	Weights for safety, phase match & steering
c_{ik} & $b_{i,n}$	k^{th} bit of Walsh code for m_i & n^{th} bit of m_i
η_m	Required data rate for m_i, $\forall i \in \{1,..,M\}$
P_i	Transmit power consumed in m_i, $\forall i \in \{1,..,M\}$
Pr^R & P^S	Received power in R & Safe transmit power
$\delta^{M-S}, \delta^{M-M}$ & σ	SNR in path M-S and M-M & Noise variance
N_o	Gaussian distributed noise P.S.D $\in (0, \sigma^2)$

locations (r_m, θ_m, ϕ_m), where $r_m \in [0, r_{max}]$ is the maximum distance of separation in muscle. Let $\theta_m \in [0, 2\pi]$ be the azimuth angle measured from the X-axis, and $\phi_m \in [0, \pi])$ be the elevation angle measured from the Z-axis, respectively, with the origin at $(0, 0, 0)$ as shown in Fig.2. The angle-units are in radians. The number of implants in a given body part can vary from 1 to M, for e.g., neural stimulation uses more than 50 implanted cuffs in one limb [1], [10]. The external relay node R on the body surface controls the actions of the implant-group by issuing synchronization pulses, aggregating their information, providing receiver feedback for beamforming and decoding the sensed values [11]. It is located at $(r_R, \theta_R, \phi_R) = (T, 0, 0)$, where T is the tissue thickness separating R and the (r, θ) plane at $\phi = \pi/2$, in which the implants are embedded. We assume identical path loss for all the implants and the tissue channel has negligible signal reflection, scattering, or shadowing [2].

● **Implant-Implant channel:** The channel between a given muscle implant (m_i) and another peer implant (m_j) that communicates along the M-M path is specified by the gain gx_{ij}^{M-M}, and phase shift ψx_{ij}^{M-M} for a field $x \in [\overrightarrow{E}, \overrightarrow{H}]$. Here, $\overrightarrow{E}$ is the electric field and $\overrightarrow{H}$ is the magnetic field. The channel gain and phase are obtained as $gx_{ij}^{M-M} = f_1^{M-M}(||r_{ij}||, \theta_{ij})$ & $\psi x_{ij}^{M-M} = f_2^{M-M}(||r_{ij}||, \theta_{ij})$ where, θ_{ij} is the relative azimuth angle between m_i and m_j, and $||r_{ij}||$ is the separation between implants (m_i) and (m_j) through the M-M path estimated as $||r_{ij}|| = \sqrt{r_i^2 + r_j^2 - 2r_i r \cos(\theta_i - \theta_j)}$. The relative elevation angle $\phi_{ij} = 0$ as the implants are assumed to be co-planar. Note the above formulation can be trivially extended for non co-planar muscle implants, though we leave out this case for space limitations.

● **Implant-Relay channel:** The channel between the implant (m_i) to relay R communication through the M-S path is given in terms of gain (gx_{iR}^{M-S}) and phase shift introduced by the tissue path through muscle-fat-skin interfaces (ψx_{iR}^{M-S}) for a field x, written as,

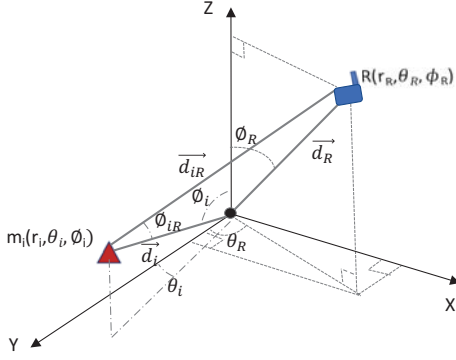$$gx_{iR}^{M-S} = f_1^{M-S}(||r_{iR}||, \theta_{iR}, \phi_{iR}) \quad \& \tag{1}$$

Fig. 2. Spherical coordinate system with an implant m_i and a relay R

$$\psi x_{iR}^{M\text{-}S} = f_2^{M\text{-}S}(||r_{iR}||, \theta_{iR}, \phi_{iR}) \tag{2}$$

where θ_{iR} and ϕ_{iR} are angles defined similarly between m_i and R. $||r_{iR}||$ is the separation between implant (m_i) and relay through the M-S path estimated as $||r_{iR}|| = \sqrt{r_i^2 + r_R^2 - 2r_i r_R [A+B]}$, where $A = sin(\theta_i)sin(\theta_R)cos(\phi_i - \phi_R)$ and $B = cos(\theta_i)cos(\theta_R)$, and $P \in \{M-M, M-S, S-M\}$ is the path of the signal. The functions $f_1^{M\text{-}M}$, $f_2^{M\text{-}M}$, $f_1^{M\text{-}S}$ and $f_2^{M\text{-}S}$ are obtained using the channel models for $\overrightarrow{E}$ and $\overrightarrow{H}$ fields in [2].

B. Near-field signal propagation

Signals impinging on a receive antenna are typically assumed to have planar wavefront. This assumption is not valid in GC-IBN for the following reasons: First, GC-IBN uses the operating frequency of $100\,\text{kHz}$ to $1\,\text{MHz}$, with a wavelength (λ) of $2E3$ to $3E3\,\text{m}$. Second, the size of the electrodes used in implants range from few μm to mm. The far-field range of such small electrodes is given by $r \geq \frac{\lambda}{2\pi}$, i.e., $r \geq 3.1E2$ for $100\,\text{kHz}$ and $4.7E2\,\text{m}$ for $1\,\text{MHz}$. However, the possible separation between the transmitter and receiver in GC-IBN can be at most $30\,\text{cm}$ based on measurements in [2]. Beyond this range, the received SNR is too low for messages to be reliably decoded. Thus, GC-IBN communication is confined to the near-field range.

Consider the electric field ($\overrightarrow{E}_i$) that is proportional to the normal component of the voltage (V_{in}) applied to the input electrodes that couple the GC signal to muscle. The magnetic field ($\overrightarrow{H}_i$) is proportional to the applied current (I_{in}) in the same implant m_i. The instantaneous $\overrightarrow{E}_i$ and $\overrightarrow{H}_i$ field strengths in the far field decrease inversely with distance (inverse-square law) and carry a relatively uniform wave-pattern, where the received signal is assumed to have constant frequency and infinite plane of constant phase and constant peak-to-peak amplitude normal to the phase velocity vector. These fields are also orthogonal to each other. As opposed to this, in the near-field, $\overrightarrow{E}_i$ and $\overrightarrow{H}_i$ field strengths falls exponentially with increasing distance from the source, contrary to the inverse-square law. Moreover, they can exist independent of each other with their field distributions depending on the tissue structure complexity without a strictly defined decreasing relationship. The electric and magnetic components expand spherically

from the electrodes and hence the received signal in the near-field can be modeled as spherical wavefront.

C. Electric field pattern based on tissue orientation

The current coupled to the input electrodes introduces an isotropic radiation pattern in the surrounding tissue. However, higher conductivity along the longitudinal axis of the muscle tissue results from the continuous muscle strands that are oriented similarly. Coupled with the layered structure of such tissues in the transverse direction, the electrical field is $\approx \sqrt{2}$ times stronger in the longitudinal direction of the muscle tissue [3]. To incorporate this tissue anisotrophy, we model the spherical wave-front of electric field ($\overrightarrow{E}_i$) and magnetic field ($\overrightarrow{H}_i$) as follows.

$$\overrightarrow{E}_i = V_{in} \times \begin{cases} sin\left(\frac{\pi}{2} - \frac{\phi}{4}\right), & \forall \phi \in [0, \frac{\pi}{2}] \\ sin\left(\frac{\frac{\phi}{4} - \pi}{2}\right), & \forall \phi \in [\frac{\pi}{2}, \pi] \end{cases} \tag{3}$$

$$\overrightarrow{H}_i = I_{in} \times \begin{cases} 1.7 - sin\left(\frac{\theta}{2} + \frac{\pi}{4}\right), & \forall \theta \in [0, \pi] \\ 1.7 - sin\left(\frac{\theta - \pi}{2} + \frac{\pi}{4}\right), & \forall \theta \in [\pi, 2\pi] \end{cases} \tag{4}$$

For the instantaneous $\overrightarrow{E}_i$ and $\overrightarrow{H}_i$ fields emanating from m_i, the instantaneous energy flux density caused in the surrounding tissue is expressed as Poynting vector: $\overrightarrow{P}_i^T = \overrightarrow{E}_i \times \overrightarrow{H}_i$, where, the real part denotes the power flow and imaginary part represents the reactive near-field of antenna. The field pattern for the implant m_i during transmission is shown in Fig. 6(a).

D. Received signal at the relay without beamforming

The received near-field signal at R due to transmissions by source m_i can be determined by modeling the propagation behavior through tissue channel independently for $\overrightarrow{E}$ & $\overrightarrow{H}$ as

$$\overrightarrow{Pr}_i^R = \overrightarrow{E_i^R} \times \overrightarrow{H_i^R} \tag{5}$$

where $\overrightarrow{E_i^R} = \overrightarrow{E}_i . ge_{iR}^{M\text{-}S} e^{j\omega\left(\psi e_{iR}^{M\text{-}S} + \gamma e_{iR}^{M\text{-}S}\right)}$, $\omega/2\pi$ is the operating frequency, $\overrightarrow{H_i^R} = \overrightarrow{H}_i . gh_{iR}^{M\text{-}S} e^{j\omega\left(\psi h_{iR}^{M\text{-}S} + \gamma h_{iR}^{M\text{-}S}\right)}$ and $\gamma_{iR}^{M\text{-}S}$ is the effect of drift in frequency and phase offset. We consider M co-planar implants transmitting simultaneously whose positions are uniformly distributed around the reference point with distribution $\frac{r_{max}}{\sqrt{2}}$. The ge and gh values for different tissue path are obtained from the HFSS based finite element simulation model in [2]. We define the term *array factor* as the net received signal pattern at the receiver resulting from multiple concurrent transmissions from the array of implants. For the $\overrightarrow{E}$ and $\overrightarrow{H}$ fields in the uniformly distributed planar implant array, the respective array factors can be written as,

$$E[AF_E] = \frac{1}{M}\sum_{i=0}^{M-1} \overrightarrow{E}_i ge_{iR}^{M\text{-}S} e^{j\omega\left(\psi_{iR}^{M\text{-}S} + \gamma_{iR}^{M\text{-}S}\right)} \quad \& \tag{6}$$

$$E[AF_H] = \frac{1}{M}\sum_{i=0}^{M-1} \overrightarrow{H}_i gh_{iR}^{M\text{-}S} e^{j\omega\left(\psi_{iR}^{M\text{-}S} + \gamma_{iR}^{M\text{-}S}\right)} \tag{7}$$

where $E(.)$ is the expected value, as the parameters are uniformly distributed values depending on the uniformly dis-

tributed position of the implants. Recall that the $\overrightarrow{E}$ and $\overrightarrow{H}$ fields are mutually independent. Hence, the array factor can be written as,

$$E[\overrightarrow{AF}] = E[\overrightarrow{AF}_E \times \overrightarrow{AF}_H] \qquad (8)$$

The resulting received signal power at the relay, due to the array effect in (8), is oriented along the muscle fiber with less energy propagating towards the relay. This pattern is plotted in polar form (azimuth and elevation planes) in Fig. 3.(a)-(b) and the power for various number of implants is plotted in Fig. 6(a)-(c)) using spherical coordinates.

E. Increased received signal at relay with beamforming

While beamforming focuses the signal energy to the relay, we must ensure that the maximum received power at any point in tissue surrounding the transmitting implant array should be less than the maximum limit (P_S). Using the motivation from our experimental study in Sec.III, we aim to minimize the phase differences among the transmitting implants and lower per-node power requirements.

We propose a conventional delay and sum beamforming method using three weights as explained below.

• **Safety weight** (w^s): Assuming the minimum required SNR for successful communication in the M-M and M-S paths to be $\delta^{M\text{-}M}$ and $\delta^{M\text{-}S}$, the minimum required transmission power by an implant (m_i) becomes:

$$P_i^{min} = \begin{cases} \dfrac{\delta_j^{M\text{-}M} N_o^j \triangle f_j}{g_{ij}^{M\text{-}M}} & \forall i,j \in \{1,..,M\} \\[3mm] \dfrac{\delta_R^{M\text{-}S} N_o^R \triangle f_R}{g_{iR}^{M\text{-}S}} & \forall i \in \{1,..,M\} \end{cases} \qquad (9)$$

where N_o^j is the Gaussian noise P.S.D received at the receiver j with zero mean and variance $\sigma^2 = 1e\text{-}8\,W/\sqrt{Hz}$, and $\triangle f_j$ is the receiver bandwidth. When the received power in the receiver exceeds the minimum requirement, the transmitting implant m_i can suitably reduce P_i to just meet the expected SNR threshold. The optimal amount of transmitted power by an implant m_i to a receiver, be it either an implant or a relay, can be chosen as:

$$P_i = \dfrac{P_{ic}}{w_{ij}^s}, \forall \in \{1,..,M\} + \{R\} \qquad (10)$$

where $w_{ij}^s = \dfrac{\delta_{jc}^{M-x}}{\hat{\delta}_j^{M-x}}$, P_{ic} is the current transmit power, δ_{jc}^{M-x} is the current SNR, $\hat{\delta}_j^{M-x}$ is the expected SNR and $x \in [M, S]$.

Note that the maximum transmission power P_i^{max} is limited by the permitted level of signal propagation through tissues as $P_i \leq P_S$. If there are multiple concurrent transmissions, then the cumulative signal at any point should also meet the safety criteria $\sum_{i=0}^{M-1} P_i \leq P_S$. Thus, for safe and energy efficient choice of transmit power, the safety weight is chosen as:

$$w_{ij}^s = max\left(\dfrac{\delta_{jc}^{M-x}}{\hat{\delta}_j^{M-x}}, \dfrac{\sum_{i=0}^{M-1} P_i}{P_S}\right), \qquad (11)$$
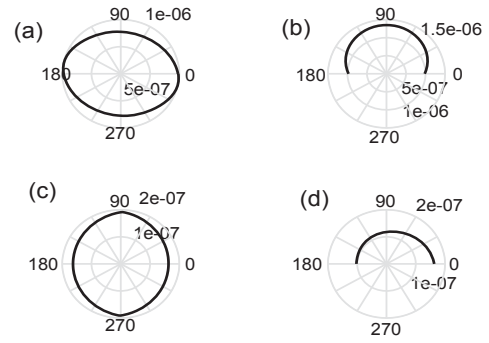

Fig. 3. Directivity of received signal before (a,b) & after (c,d) beamforming

$\forall i \in \{1,..,M\}$ & $\forall j \in \{1,..,M\} + \{R\}$. Using w_{ij}^s, the magnitude of P_i can be estimated using (10).

• **Phase-match weight** (w_{ij}^p): As seen in Fig. 6(c), the mismatch in phase among the signals results in destructive signal combination, and thus, reduces the net received power. To perfectly synchronize the uniformly distributed planar implant array, we first match the link-dependent phase shift of each implant obtained in (2) with respect to the reference position at (O). Then, using the excellent cross-correlation property of the Walsh codes that we use later in Sec. V, we extract the phase differences from the frequency offsets iteratively as $\gamma' h_{iR}^{M-S}$ and compute the overall phase lag of each implant in the form of Phase match weight as:

$$w_{ij}^p = \psi h_{iR}^{M-S} + \gamma' h_{iR}^{M-S} \qquad (12)$$

• **Steering weight** (w^t): This weight allows steering the signal from the transmitter to the relay with the desired beam shape given in Fig. 3.(c)-(d). In the desired beam, along the elevation plane in Fig. 3.(d), the beam power is increased at $\phi=0$ towards the position of the relay and in the azimuth plane in Fig. 3.(c), the propagation is steered away from the neighbors at $\theta=0, \pi$. The corresponding steering weight is given as:

$$w_{iR}^t = sin(k\theta_{iR})cos(k\phi_{iR}) + sin(k\theta_{iR})sin(k\phi_{iR}) \qquad (13)$$

where, θ_{iR} and ϕ_{iR} are the respective relative azimuth and elevation angles, respectively, between the implant and relay (refer Fig.2), $k = \frac{2\pi f}{c'}$ is the wave number, c' is the propagation speed of signal through the tissue medium estimated using the permittivity of the medium as,

$$c' = c/\sqrt{\epsilon}\ m/s \qquad (14)$$

where c is propagation speed of light in vacuum and ϵ is the permittivity of the medium. c' for muscle is around $9.5e6\ m/s$ and that of skin is around $8.3e6\ m/s$.

We adjust the array factor of the $\overrightarrow{H}$ field in (7) using the three weights derived above as,

$$E[AF_H] = \dfrac{1}{w_{iR}^s M} \sum_{i=0}^{M-1} \overrightarrow{H}_i g h_{iR}^{M\text{-}S} e^{j\omega\left(\psi_{iR}^{M\text{-}S} + \gamma_{iR}^{M\text{-}S}\right)} e^{w_{iR}^t - w_{iR}^p} \qquad (15)$$

The average power pattern of the uniformly distributed planar array can be estimated as $E[|AF|] = |AF|(1 - \frac{1}{M}) + \frac{1}{M}$. We use our simulation environment to study the maximum
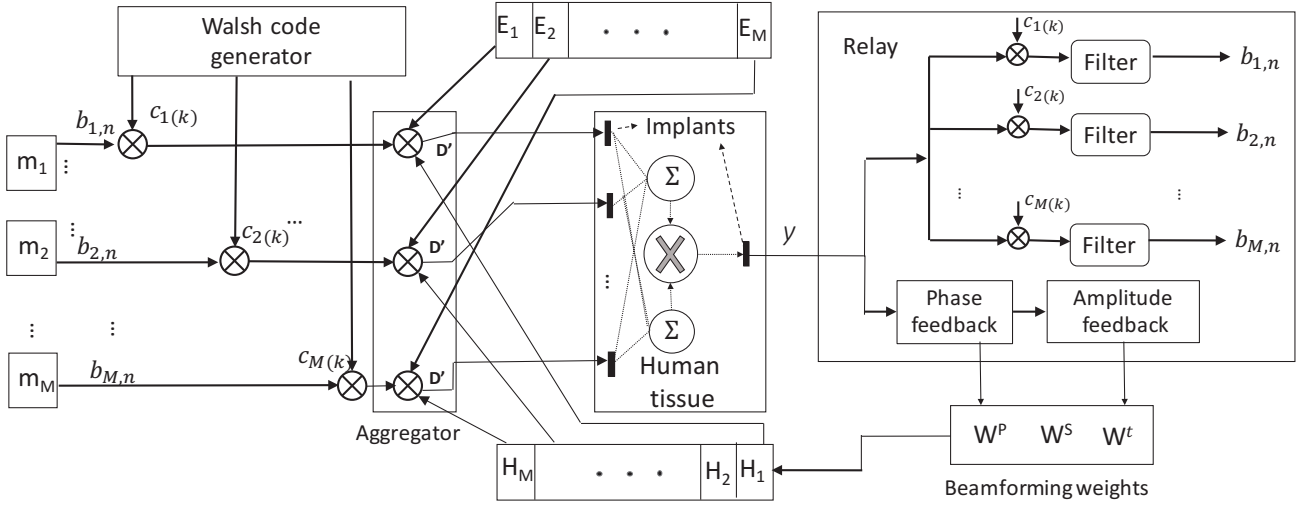
Fig. 4. CDMA & beamforming based MAC framwork for implants communication using GC-IBN

power level in the tissue area using

$$P^{max} = max_{\{r,\theta,\phi\}} E[\|AF\|] \qquad (16)$$

V. BEAM FORMATION USING CDMA

The orthogonal CDMA codes distributed by the relay to implants play a critical role in facilitating beamforming; it helps in creating a common data vector in each implant as well as solves the problem of instantaneous transmissions by multiple implants in case of sudden abnormalities. The beam formation and the process of end-to-end data communication is split into four phases, as described below (see Fig. 5):

● **Stage I. Resource assignment by the relay:** Each communication cycle starts a parameter setting beacon by the relay that allows implants to synchronize, set duty cycles for peer-level and beamforming-based communication, use orthogonal CDMA Walsh codes to partition the collision domain, and compute feedback weights for the array factor given in (11), (12) and (13) for optimal beamshaping (refer stage.1 in Fig.5). Communication from implants are acknowledged in a successive round, enabling the implants to sleep immediately after they transmit the beam. Since we require each implant to have a common data vector prior to beamforming, the relay also appoints an aggregator (ID_A) for the next round of communication. The aggregator's role is simply to collect the individual and simultaneously transmitted spreaded sequences that combine in the tissue channel, and save this as the common data vector. The aggregator is a peer-implant, and its role is rotated in every round.

● **Stage II. Peer communication phase:** The relay provides synchronized slots (T_B) for all implants to combine their data using the Walsh codes and transmit them simultaneously. This transmission is intentionally set to very low power given that it traverses the high-gain M-M path to the aggregator node (refer stage.2 in Fig.5). The spreading factor of the code is chosen based on the number of implants. The implant ID is associated with a unique spreading code sequence c_i among all the CDMA codebook. For N data bits of the implant, each bit is directly multiplied by the Walsh code with L elements

(refer Fig. 4) to form the spread sequence $b_{i,n}c_i$, $\forall\ i\ \in \{1,..,M\}$, $n\ \in\ \{1,..,N\}$ of size $L\times 1$. These orthogonal Walsh codes have excellent cross correlation properties that enable simultaneous non-interfering transmissions. After spreading at the sampling time instant corresponding to the index k, $\forall k \in \{0,..,L-1\}$, the implants transmit the spreaded sequence b_ic_i through the M-M path. At this stage, neither other implants nor the aggregator performs any decoding. Note that an implant can opt out of transmission in a cycle and sleep for prolonged period if its sensing cycle is longer. Also, the M-M communication is not strictly synchronized that relieves the implants from complex scheduling and mutual phase offset computation for this first round of messaging. An implant can choose to transmit anytime between the allowed window of peer-level M-M communication.

The aggregator receives the sequence $\mathbf{D}$ as a vector of size $L\times 1$ from the $M-1$ implants as,

$$\mathbf{D} = \sum_{i=1}^{M-1} g_{iA}^{(M-M)} b_{i,n}\mathbf{c}_i + \mathbf{w} \qquad (17)$$

where A represents the aggregator, $b_{i,n}$ is the n-th bit sent by the implant m_i, $\mathbf{c}_i = [c_i(0), c_i(1),...,c_i(L-1)]^T$ is the spreading code for m_i, T denotes the transpose and $\mathbf{w}$ is the iid additive white Gaussian noise vector with zero mean and variance σ^2 of size $L\times 1$ given by $[w(k-L+1), w(k-L+2),...,w(k)]^T$. Since each implant transmits in a narrow band channel ($100\ kHz$) the M-M channel can be represented as a single tap channel [2]. We assume that $g_{ij}^{(M-M)}$ is constant during a transmission cycle.

Once the aggregator receives the overall CDMA vector containing the spread data, it sends back the common CDMA vector ($\mathbf{D}$) representing the aggregated value to the peer implants through a single broadcast, again using the high-gain M-M path. The spread data received back at the i-th implant can be expressed as

$$\mathbf{D}'_i = g_{Ai}^{(M-M)}\mathbf{D} + \mathbf{w} \qquad (18)$$
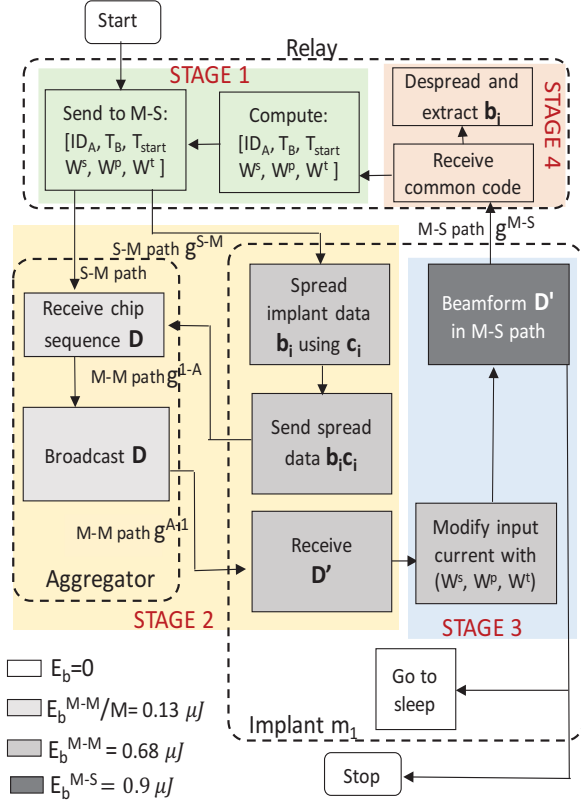
6

Fig. 5. Stages showing the entire end-to-end implant to relay communication

Now, all the implants have the common CDMA vector $\mathbf{D}'$, which may only slightly differ from each other depending on the channel coefficient of the M-M path from the aggregator to the specific implant according to (18).

● **Stage III. M-S Beamforming phase:** In this phase, each implant acts as an independent antenna array element and attempts to form a beam sending the same overall CDMA data vector that has been shared with all the implants at the instant T_B predetermined by relay. The use of the same CDMA data during beamforming further improves the SNR and lowers the required M-S transmission power at the implants as shown in Sec.IV. Although each implant acts as an element of a virtual antenna array sending the same information, the individual implant signals differ in amplitude and phase, as instructed by the beamforming weights. The implants tune their transmission based on the weights, such that all the transmissions from implants constructively amplify the received signal $\mathbf{y}$ at the relay and maximize the received power.

Thus, each implant sends the information at lower power compared to individual transmissions in the M-S channel, enabling significant energy savings. The received vector at the relay is given by

$$\mathbf{y} = \sum_{i=0}^{M-1} S_i \mathbf{D}'_i + \mathbf{w} \tag{19}$$

where $S_i = \frac{1}{w_{iR}^s M} g h_{iR}^{M\text{-}S} e^{j\omega\left(\psi_{iR}^{M\text{-}S} + \gamma_{iR}^{M\text{-}S}\right)} e^{w_{iR}^t - w_{iR}^p}$ obtained from (15) that accounts for both the steering coefficient of

the implant m_i and the channel coefficient of the M-S path from the implant m_i to the relay R on surface. The implants enter into the sleep state immediately after sending the beam until the next transmission cycle (see stage.3 in Fig. 5).

● **Stage IV. Despreading and feedback at the relay:** Having received the common CDMA vector through the beamformed signal, the relay despreads the signals using a matrix with the same Walsh codes distributed to the individual implants. In this way, it recovers the sensed data and the associated ID of each implant, as shown in Fig. 4. The despreading uses the cross-correlation of the received signal $\mathbf{y}$ with the known Walsh codes as follows

$$\hat{b}_{i,n} = \mathbf{y}^T \mathbf{c}_i \tag{20}$$

At the relay, the signal-to-interference-plus-noise power ratio (SINR) is given by [12]:

$$SINR = \left(\frac{N_0}{E_s} + \frac{M-1}{G}\right)^{-1} \tag{21}$$

where E_s is the energy per symbol, G is the spreading factor, and M is the number of concurrent transmissions, corresponding to the number of implants. The bit error rate (BER) can be computed from the $SINR$ as

$$BER = \frac{1}{2} erfc(\sqrt{SINR}) \tag{22}$$

In terms of transmission and propagation time, the whole transmission cycle takes

$$4\frac{L}{\eta} + 2\frac{\psi x_{iR}^{M\text{-}M} + \gamma x_{iR}^{M\text{-}M}}{360f} + 2\frac{\psi x_{iR}^{M\text{-}S} + \gamma x_{iR}^{M-S}}{360f} + 4T_R \tag{23}$$

seconds, where L is the frame (or chip) length and T_R is the tissue relaxation time required between transmissions to assure normal tissue temperature under abnormal blood flow rates, calculated as $T_R = \sqrt{\frac{\epsilon}{\sigma}}$, ϵ & σ being the tissue permittivity and conductivity.

Finally the relay computes the weights w_{iR}^s, w_{iR}^p and w_{iR}^t using (11), (12) and (13) for the successive transmission and transmits them to the implants at the predetermined interval as given in stage.1 in Fig. 5.

VI. PERFORMANCE EVALUATION & RESULTS

In this section, we evaluate the energy savings achieved by the proposed CDMA based beamforming framework by (i) analyzing the proportion of energy propagating in the direction of the relay to that leaking in the undesired directions, (ii) studying the influence of the number of array elements on the implant power consumption, (iii) quantitatively measuring the improvement in implant lifetime, and (iv) comparing the energy consumption for the overall M-S path communication with/without our approach. We develop a 3-D multi-layer, heterogeneous tissue channel model in MATLAB, operating at a narrow band of $100\ kHz$. The tissue area has the dimension of 20×20cm, with r_{max}=20 cm. The separation between the layer of implants in muscle and the surface is 2.2 cm. The maximum safe transmit power is 1 mW.
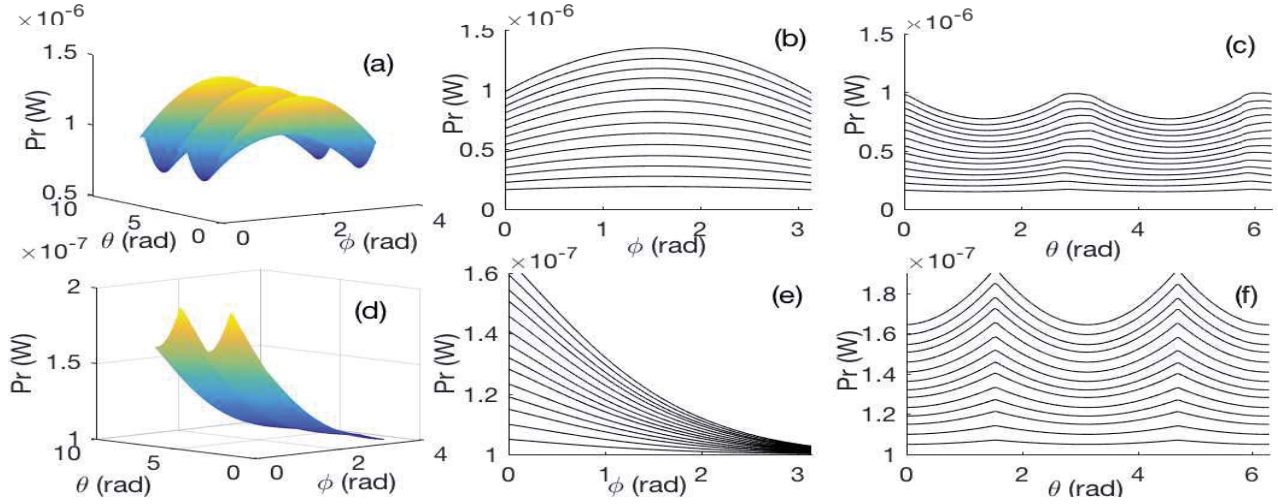
Fig. 6. Received power before and after beamforming

A. Effectiveness of beamforming

The pattern of received power at the relay resulting from the sum of the signals concurrently propagating through the tissue medium without beamforming is shown in Fig. 6(a)-(c). Here, the propagation is oriented towards the longitudinal muscle direction (at $\phi=\frac{\pi}{2}$, $\theta=0,\pi$), where more energy flow occurs along the length of the arm. This causes minimal flux at the surface relay (at transverse direction at $\phi=0$). This pattern may also cause more interference to the potentially neighboring implants (refer Fig. 1(left) for the direction of neighbors). Before beamforming, the ratio of energy flow in the required direction to undesired direction is ≈ 0.53. Fig. 6(d)-(f) shows the received signal at relay after beamforming, where more power is steered towards the relay (at $\phi=0$) and there is less power in the longitudinal direction ($\phi=\frac{\pi}{2}$, $\theta=0,\pi$) mitigating the interference to neighbors.

Fig. 6(b)-(c) shows power degradation when signals with different phases are combined together. After the phase mismatch is rectified using W^p in the beamforming process, the signals add up constructively (refer Fig. 6(e)-(f)) as demonstrated in Fig. 1(d) and improve the received power by an additional $\approx 3\%$ as shown in Table.II as $Pr(W^p)$. Note that this is the received power obtained after the transmit power is reduced to sufficient level using w^s weight. We analyze the maximum induced power at every point in the given tissue area defined by θ, ϕ and r using (16) and verify that the cumulative received power at any point in the tissue with multiple concurrent transmissions does not exceed the restrictions posed by safety limits, confirming the tissue safety and normal thermal distributions [4]. Using the simulation environment, we further ensure that $\int_\theta \int_\phi \int_r Pr dr d\phi d\theta \leq 25 \frac{mA}{m^2}$.

Influence of number of implants: The resulting proportion of power in the required to undesired direction is plotted in Fig. 7.(a) illustrating that more power is steered towards the relay when there are more number of implants forming the array. Thus both the critical beamforming parameters namely, the per implant power conservation and the directivity of beamforming, are improved with the number of implants or

array elements (M). The actual SNR for individual transmission from each implant through M-S path is compared with the exponential increase in SNR at the receiver after beamforming with M implants in Fig. 7(b).

Implant lifetime: The transmission power of the implants is reduced to just meet the required SNR by applying the safe weight w^s derived in (11). The resulting power consumed (aPt) in each implant vs M and the corresponding improvement in implant lifetime is shown in Table.II. We see that the implant life dramatically extends from 10 weeks when used without beamforming, to ≈ 138 weeks with beamforming for the scenario with 14 implants.

B. BER & energy analysis for CDMA-beamforming

The proposed CDMA scheme allows concurrent simple transmissions for the implants. There is, however, an additional overhead of (i) spreading the data using the Walsh codes, and (ii) (albeit high gain M-M) communication between implants to the aggregator and back. We aim to study whether this cost is offset by the energy savings achieved by beamforming.

The CDMA performance without the beamforming is shown in terms of BER computed using (21)-(22) in Fig. 8(a). For N_o=1e-8 and the receiver bandwidth of $1e3\,Hz$, the maximum SNR obtained is 0.92 for a single transmitter. This SNR gets worse with multiple CDMA transmissions resulting in poor BER. However, the CDMA solution performs better with dramatically improved BER when using beamforming contributed by the improved SNR at the relay, i.e., E_s/N_0 in (21)
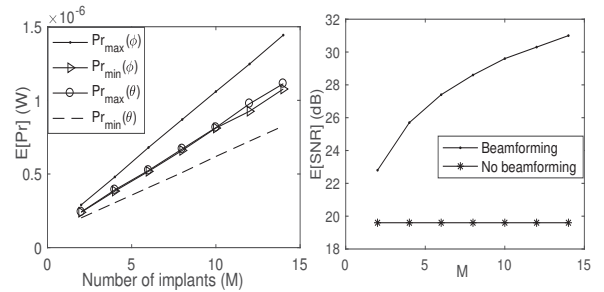

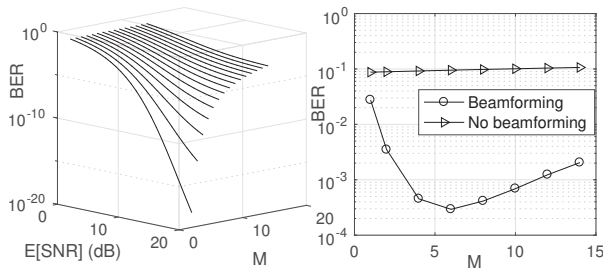Fig. 7. (a) Directionality (b) SNR before & after beamforming

Fig. 8. (a) CDMA BER performance (b) Comparison of CDMA with and without beamforming

reduces the BER according to (21)-(22). This is illustrated in Fig. 8(b). For the given scenario, the BER improves from 0.18 for one implant upto $1.5e$-4 for six implants. For $M>6$, the BER starts to decline with M, showing that the advantage of beamforming is more effective for a low number of implants in array. For a high number of concurrent implant transmissions, the interference effect $\frac{M-1}{G}$ in (21) becomes dominant, pulling down the performance.

Network traffic and time: With the proposed framework with L=64, the total traffic flow in a transmission cycle becomes 32 bytes, which is much lower than the existing IEEE 802.15.6 standard that requires a minimum of 13×4 bytes as frame header alone not including the data. The time required for the whole transmission cycle is estimated using (23) for T_R=10 μs and η=100 $kbps$ to be only 1.3 ms that is mainly dominated by the transmission time.

With and without beamforming: We next compare the energy consumption for the implant to relay communication through the M-S path with and without the beamforming. For an expected link length of 5 cm, the average M-S pathloss is 41.2 dB. The energy per bit required for a desired SNR of $\hat{\delta}$ is given using (9) by E_b=P_i^{min}/η. For $\hat{\delta}$=10, a noise factor (N_o) of $1e$-8, data rate η of 10 $kbps$ and bandwidth $\triangle f$ being $1e5$ Hz, the required energy per bit (E_b) becomes 6.62 μJ. This would allow battery of capacity of 240 mAh to last for 2.89 years.

Before beamforming, the implants first broadcast their individual codewords in the M-M path. This step requires an energy of 0.68 μJ, considering the same values as assumed above for all other parameters, other than the lower path loss through M-M path (19 dB). The aggregated codeword is then transmitted from the aggregator as a broadcast to all implants that requires $\approx 0.7 \mu J$. Finally, the beamforming towards the relay is undertaken in the M-S path, where each node spends

TABLE II
POWER CONSUMPTION FOR 1 BIT WITH $E[P] = 0.5mW$

M	Pr (μW)	$Pr(W^p)$ (μW)	aPt (mW)	Life (weeks)
1	0.9	0.92	0.5	10
2	1.9	1.93	0.23	21
4	3.67	3.71	0.12	40
6	5.37	5.49	.085	59.5
10	8.94	9.11	0.05	98.8
14	12.4	12.7	0.03	137.9

about $4e$-$5M^{-1.03}$ times less energy than that actually required for the direct M-S path. For a scenario with 4 implants, the power consumption in each implants for the complete transmission cycle is 1.39 μJ, which is 4.7 times lower than that required for M-S communication without beamforming. The proposed framework extends the life of implant upto 13.8 years assuming every other parameter remains the same.

VII. CONCLUSION

In this paper, we propose an energy efficient implant to surface relay communication using galvanic coupling that uses beamforming. The proposed communication technique is strongly focused on improving energy efficiency by: sharing sensed updates among peer-implants using CDMA codewords through the high-gain M-M path, avoiding unpredictable data delivery conditions caused by collisions and transmission back-offs. Then, through near-field beamforming performed by the implants organized into distributed transmitter arrays, communication through the vertical tissue layers is achieved with high SNR (or conversely, lower energy per implant). The proposed framework dramatically lowers the net energy required for end-to-end implant to relay communication that is 79% more energy efficient than the direct case, and extends the lifetime of implants upto 13 years.

REFERENCES

[1] E. Strickland, "Cyborgs go for gold," *IEEE Spectrum*, vol. 53, no. 1, pp. 30–33, 2016.
[2] M. Swaminathan, F. S. Cabrera, J. S. Pujol, U. Muncuk, G. Schirner, and K. R. Chowdhury, "Multi-path model and sensitivity analysis for galvanic coupled intra-body communication through layered tissue," *IEEE transactions on biomedical circuits and systems*, vol. 10, no. 2, pp. 339–351, 2016.
[3] K. Hoyt, B. Castaneda, and K. Parker, "5c-6 muscle tissue characterization using quantitative sonoelastography: Preliminary results," in *IEEE Ultrasonics Symposium*, Oct 2007, pp. 365–368.
[4] P. Vecchia et al., "Exposure to high frequency electromagnetic fields, biological effects and health consequences (100 kHz-300 GHz)," *International Commission on Non-Ionizing Radiation Protection*, 2009.
[5] I. S. Association *et al.*, "802.15.6-2012 IEEE standards for local and metropolitan area networks–part 15.6: Wireless body area networks."
[6] C. Van Phan et. al., "An energy-efficient transmission strategy for wireless sensor networks," *IEEE Transactions Consumer Electronics*, vol. 56, no. 2, pp. 597–605, 2010.
[7] Jui-Yuan Yu et al., "A MT-CDMA based wireless body area network for ubiquitous healthcare monitoring," *IEEE BioCAS Conference*, pp. 98–101, 2006.
[8] J. D. et al., "Energy-efficient distributed beamforming in uwb based implant body area networks," *IEEE VTC*, 2015, pp. 1–5.
[9] J. F. Alfaro, "A multi axial bioimplantable mems array bone stress sensor," Ph.D. dissertation, Citeseer, 2007.
[10] P. Strojnik and P. H. Peckham, "Implantable stimulators for neuromuscular control," *The Biomedical Engineering Handbook, 2nd edn. CRC Press LLC, Boca Raton*, 2000.
[11] M. Swaminathan, U. Muncuk, and K. R. Chowdhury, "Topology optimization for galvanic coupled wireless intra-body communication," *IEEE INFOCOM 2016*, April 2016.
[12] A. Goldsmith, *Wireless Communications*, 2005.